

# Charged Higgs Contribution into $t\bar{b}$ -pair Production in Hadronic Collisions

M.V. Foursa<sup>1</sup>, D.A. Murashov<sup>2</sup> and S.R. Slabospitsky<sup>3</sup>

*State Research Center  
Institute for High Energy Physics,  
Protvino, Moscow Region 142284  
RUSSIA*

## Abstract

We investigate the charged Higgs boson contribution into  $t\bar{b}$ -pair production in  $pp$ -collisions at LHC. It is shown that due to the  $H^\pm$ -boson exchange the total yield of  $t\bar{b}$  is modified significantly for small and large values of  $\tan\beta$ . However, for the small values of  $\tan\beta$  one should expect also the production of right-handed top quark contrary to pure left-handed  $t$ -quark production through  $W^\pm$ -boson exchange only. This fact provides the possibility to separate  $H^\pm$  and  $W^\pm$  contributions by means of the investigations of angular distributions of top decay products. The detailed simulation of the signal and relevant background processes is performed.

Protvino, 2000

---

<sup>1</sup> fursa@mx.ihep.su,

<sup>2</sup> murashev@mx.ihep.su,

<sup>3</sup> slabospitsky@mx.ihep.su

# 1 Introduction

The existence of the charged Higgs boson  $H^\pm$  is predicted by many extensions of the Standard Model (see, for example, [1]). The search for charged Higgs boson is carried out in  $e^+e^-$  annihilation at LEP-2 collider at CERN [2] as well as at the Tevatron in the top quark decays [3]. The search of the  $H^\pm$ -boson will be one of the main experimental task at future LHC machine [5, 4]. The main channels for  $H^\pm$ -boson search are the reactions of  $gb \rightarrow tH^-$  and  $gg \rightarrow t\bar{b}H^-b$  [5, 6, 7].

In the present article we consider the additional possibility for study of a signal from charged Higgs boson in the quark-antiquark annihilation subprocess:

$$q\bar{q}' \rightarrow H^+ \rightarrow t\bar{b} .$$

Namely, we consider the charged Higgs boson contribution to the process of  $t\bar{b}$ -pair production in proton-proton collisions

$$pp \rightarrow t\bar{b} X. \quad (1)$$

Note, that  $t\bar{b}$  quark production though  $W$ -boson exchange in the  $s$ -channel had been considered earlier (see [4, 8, 9, 10]). This reaction plays a significant role in study of electroweak  $t$ -quark production. In particular, this process is very important for the investigations of the electroweak vertex of  $tWb$  interactions [4].

The New Physics beyond the Standard Model (SM) may modify the nature of  $t$ -quarks interactions (see [4] and references therein). In particular, the contribution of charged Higgs boson into the process (1) may be considered as manifestation of the New Physics. The existence of the  $H^\pm$ -boson leads not only to modification of the total cross section for  $t\bar{b}$ -pair production, but also to change of angular distributions of top quark decay products. The detailed consideration of the contribution due to several forms of the New Physics into  $t\bar{b}$ -pair hadronic production as well as the analysis of the top quark polarization properties resulted from such new interactions can be found, for example, in [10].

In the present article we investigate in details the charged Higgs boson production in proton-proton collisions at future CERN LHC machine at the energy of  $\sqrt{s} = 14$  TeV. Certainly, the strategy for search for  $H^\pm$ -boson production is determined, in particular, by the Higgs boson mass (see [5]). For relatively light  $H^\pm$ , say for  $m_{H^\pm} < m_t$ , the most promising possibility is the investigation of  $t$ -quark decay into  $H^\pm$  and  $b$ -quark. In the present article we assume, that charged Higgs is heavier than top quark. As a result we consider the top quark decays into  $W^\pm b$  pair. Moreover, we consider only leptonic decays of  $W^\pm$ -boson, because for hadronic  $W^\pm$  decays it is very difficult to separate a signal from huge QCD background.

Note, that typical differential distributions ( $p_T$  and  $\eta$ ) of the  $t$ -quark and its decay products are practically the same as for the SM production of  $t\bar{b}$ -pair (via  $W^+$ -boson exchange only). Therefore, for a separation of the  $H^\pm$  contribution we explore

$t$ -quark polarization properties, which are different for  $W^+ \rightarrow t\bar{b}$  and  $H^+ \rightarrow t\bar{b}$  contributions for small values of  $\tan \beta$ . We find the specific kinematic cuts, which provide a separation of  $H^\pm$  and  $W^\pm$  contributions in the reaction (1).

The article is organized as follows. In the Section 2 we present the explicit form of the matrix elements squared for the considered process. The behavior of the total cross section production of  $t\bar{b}$ -pair as a function of  $m_H$  and  $\tan \beta$  is considered in the Section 3. The differential distributions on  $p_T$  and  $\eta$  as well as the angular distributions of top decay products are also discussed in this Section. The detailed simulation of the signal and relevant background processes is given in the Section 4. The main results are summarized in the Conclusion.

## 2 Matrix elements calculations

The Lagrangian describing the  $\bar{t}H^\pm b$ -vertex in two doublet Higgs model has the following form [1, 5, 4]:

$$\mathcal{L} = \sqrt{\frac{G_F}{\sqrt{2}}} H^+ \{ \tan \beta \bar{U}_L V_{ij} M_D D_R + \cot \beta \bar{U}_R M_U V_{ij} D_L + \tan \beta \bar{N}_L M_L L_R \}, \quad (2)$$

where the symbols  $U$  and  $D$  refer to 'up' and 'down'-type quarks, while  $N$  and  $L$  correspond to charged lepton and neutrino,  $V_{ij}$  is Cabibbo-Kobayashi-Maskawa matrix element,  $M_D$  and  $M_U$  are the quark masses, and  $M_L$  is the mass of charged leptons,  $\tan \beta$  is the ratio of values of vacuum expectation value for two Higgs doublets,  $G_F$  is the Fermi constant.

The subprocesses of  $t\bar{b}$ -pair production through  $W^\pm$  and  $H^\pm$  exchange,

$$q_1 \bar{q}_2 \rightarrow (H^+ + W^+) \rightarrow t\bar{b}, \quad (3)$$

is described by two diagrams, presented in Fig. 1.

The corresponding matrix element squared is presented as a sum of three terms, corresponding to  $H^\pm$ -boson ( $M_H$ ) and  $W^\pm$ -boson ( $M_W$ ) exchanges and their interference ( $M_I$ ):

$$|M_{2 \rightarrow 2}|^2 = |M_H|^2 + |M_W|^2 + |M_I|^2, \quad (4)$$

where

$$\begin{aligned} |M_H|^2 &= \frac{16G_F^2 |V_{12}|^2 |V_{tb}|^2}{(\hat{s} - m_H^2)^2 + \Gamma_H^2 m_H^2} \left[ (m_t^2 \cot^2 \beta + m_b^2 \tan^2 \beta) (p_t p_b) - 2m_b^2 m_t^2 \right] \\ &\quad \times \left[ (m_1^2 \cot^2 \beta + m_2^2 \tan^2 \beta) (p_1 p_2) - 2m_1^2 m_2^2 \right], \\ |M_W|^2 &= \frac{128m_W^4 G_F^2 |V_{12}|^2 |V_{tb}|^2}{(\hat{s} - m_W^2)^2 + \Gamma_W^2 m_W^2} (p_t p_2)(p_b p_1), \end{aligned}$$

$$|M_I|^2 = \frac{32G_F^2|V_{12}|^2|V_{tb}|^2m_t m_b A}{A^2 + B^2} \times [-m_1^2 \cot^2 \beta(p_t p_2) + m_2^2(p_t p_1) + m_1^2(p_b p_2) - m_2^2 \tan^2 \beta(p_b p_1)],$$

where  $\hat{s}$  is the total energy squared of colliding partons,  $V_{ij}$  is Cabibbo-Kobayashi-Maskawa matrix element,  $\Gamma_H$  is  $H^+$ -boson decay width,  $m_i$  and  $p_i$  are the quark masses and 4-momenta respectively,  $m_W$  and  $\Gamma_W$  are the W-boson mass and decay width,  $A = (\hat{s} - m_W^2)(\hat{s} - m_H^2) + \Gamma_W m_W \Gamma_H m_H$ ,  $B = (\hat{s} - m_W^2)\Gamma_H m_H - (\hat{s} - m_H^2)\Gamma_W m_W$ .

Bearing in mind the study of the  $t$ -quark polarization properties in the reaction (1) we perform also the calculations of the subprocesses (3) with the consideration of further top quark decay. Namely, we calculate the matrix element squared for the subprocess  $2 \rightarrow 4$ :

$$q_1 \bar{q}_2 \rightarrow (H^+ + W^+) \rightarrow \bar{b}t(\rightarrow bW^+) \rightarrow b\bar{b}l^+\nu_l \quad (5)$$

Similarly to the subprocesses (3) we present the  $|M_{2 \rightarrow 4}|^2$  as a sum of three terms corresponding to the  $H^\pm$  and the  $W^\pm$  exchanges and their interference:

$$|M_{2 \rightarrow 4}|^2 = |M_H|^2 + |M_W|^2 + |M_I|^2, \quad (6)$$

where

$$\begin{aligned} |M_H|^2 &= \frac{2048m_W^4 G_F^4 |V_{tb}|^4 |V_{12}|^2 (p_b k_1)}{((\hat{s} - m_H^2)^2 + \Gamma_H^2 m_H^2) C_W C_t} \\ &\quad \times \{(q_1, q_2)[m_1^2 \cot^2 \beta + m_2^2 \tan^2 \beta] - 2m_1^2 m_2^2\} \\ &\quad \times \{m_b^2 \tan^2 \beta [2(k_2 p_t)(p_{\bar{b}} p_t) - (k_2 p_{\bar{b}}) p_t^2] \\ &\quad + m_t^4 \cot^2 \beta (k_2 p_{\bar{b}}) - 2m_b^2 m_t^2 (k_2 p_t)\}, \\ |M_W|^2 &= \frac{8192m_W^8 G_F^4 |V_{tb}|^4 |V_{12}|^2 (p_b k_1)(p_{\bar{b}}, q_1)}{((\hat{s} - m_W^2)^2 + \Gamma_W^2 m_W^2) C_W C_t} \\ &\quad \times [2(q_2 p_t)(k_2, p_t) - (q_2 k_2) p_t^2], \\ |M_I|^2 &= \frac{4096m_W^6 G_F^4 |V_{tb}|^4 |V_{12}|^2 A m_1 m_2}{(A^2 + B^2) C_W C_t} \\ &\quad \times \{m_t^2 \cot^2 \beta [(q_1, p_{\bar{b}})(p_t k_2) + (q_1 p_t)(p_{\bar{b}} k_2) - (q_1 k_2)(p_{\bar{b}} p_t)] \\ &\quad + m_t^2 [(q_2 k_2)(p_{\bar{b}} p_t) - (q_2 p_{\bar{b}})(p_t k_2) - (q_2, p_t)(p_{\bar{b}}, k_2)] \\ &\quad + m_b^2 \tan^2 \beta [2(q_2 p_t)(p_t k_2) - (q_2 k_2) p_t^2] \\ &\quad + m_b^2 [(q_1 k_1) p_t^2 - 2(q_1 p_t)(p_t k_2)]\}, \end{aligned}$$

where  $A$  and  $B$  is defined in (4);  $C_W = (p_W^2 - m_W^2)^2 + \Gamma_W^2 m_W^2$  and  $C_t = (p_t^2 - m_t^2)^2 + \Gamma_t^2 m_t^2$ ,  $p_W$  and  $p_t$  are the momenta of top quark and W-boson, respectively;  $k_1$  and  $k_2$  are the momenta of neutrino and charged lepton.

Note, that the matrix element squared (6) corresponding to the subprocess (5) is calculated for the first time.

### 3 Total cross sections and differential distributions

In our calculations we use the parton distributions from [15]. The evolution parameter  $Q^2$  is chosen to be  $Q^2 = \hat{s}$ , where  $\hat{s}$  is the total energy squared of colliding partons. In our calculations we use the following values of the  $b$  and  $t$ -quark masses

$$m_b = 4.5 \text{ GeV} \quad [16] \quad \text{and} \quad m_t = 173.8 \text{ GeV}. \quad (7)$$

For the fixed value of the charged Higgs boson mass the largest cross section is expected at large and small values of  $\tan\beta$ . The behavior of the cross section for the reaction (1) as a function of the  $H^\pm$ -boson mass and  $\tan\beta$  is presented in Fig. 2. Note, that the cross section reaches its maximum at  $m_H \sim 200$  GeV due to the pole character of cross section under consideration (see (4)).

The  $H^\pm$ -boson contribution into the reaction (1) leads to increasing of the  $t\bar{b}$ -pair cross section production. However, the modification of the "observable" number of events,  $N_{ev}(Wb\bar{b}) \sim \sigma(t\bar{b}) \times B(t \rightarrow bW^+)$ , depend on  $m_{H^\pm}$ . For the  $H^\pm$ -boson lighter than top quark ( $m_{H^\pm} < m_t$ ) the branching fraction of  $t \rightarrow bW$  decay ( $B(t \rightarrow bW)$ ) may significantly decrease [5, 4]. As a result, we should expect the decrease of  $N_{ev}$  as compared to the SM case. For heavy  $H^\pm$ -boson ( $m_{H^\pm} > m_t$ ) there is no  $t \rightarrow bH^+$  decay channel. Therefore, one has  $B(t \rightarrow bW^+) \approx 1$  and we should expect the increase of  $W^+ b\bar{b}$  yield.

The "experimentally seen" cross sections for  $t$ -quark production in the reaction (1), i.e.

$$\sigma(pp \rightarrow \bar{b}t(\rightarrow bW)X) = \sigma(pp \rightarrow t\bar{b}X) \times B(t \rightarrow bW) \quad (8)$$

are presented in the Fig. 3 for two values of  $m_H = 90$  and 200 GeV. Note, that for the small and large values of  $\tan\beta$  the  $H^\pm$ -boson contribution leads to noticeable modification of the  $t\bar{b}$ -pair production, while for the intermediate range of  $\tan\beta = 0.8 \div 20$  the  $H^\pm$  contribution becomes negligible. The differential distributions of the final particles ( $t, W, b, l$ ) on transverse momentum and pseudorapidity calculated at the parton level are shown in Figs. 4, 5. As is shown in figures, the differential distributions for the cases of  $H^+$  and  $W^+$  exchange have practically the same shapes. Therefore, the contribution of the New Physics may lead only to a deviation of the expected number of events. Therefore, to elucidate the nature of possible deviation from the SM predictions one needs to examine the additional quantities which have differential behavior for the SM and beyond SM cases.

For this purpose we explore the polarization properties of the  $t$ -quark, widely considered in the literature (see, for example, [4, 11, 12] and references therein). It is well known that the subprocess (3) leads to the production of almost left-handed  $t$ -quark [4, 10]. At the same time the charged Higgs boson contribution leads to

production of the right(left)-handed  $t$ -quark for small (large) values of  $\tan\beta$  (see [5]). Note, that for the left-handed  $t$ -quark the  $b$ -quark (the charged lepton) should flight mostly along-side (opposite) to the direction of the top quark momentum [4, 10]. Naturally, for the right-handed top quark one has the reverse situation.

Hereafter, in order to separate the  $W^\pm$  and  $H^\pm$  contributions we examine the angular distributions,

$$\frac{dN}{dcos\theta^*}, \quad (9)$$

where  $\theta^*$  is the angle in the top quark rest frame between the momenta of  $t$ -quark and final particle from the top quark decay  $t \rightarrow bl\nu$ .

In the Fig. 6 we present the corresponding angular distributions of the  $b$ -quark and charged lepton from  $t$ -quark decay calculated by means of the matrix element (6) separately for only  $W^+$  or  $H^\pm$  exchange (see the histograms "a, b, e, f" in the Fig. 6). For evaluating of these distributions we set  $m_{H^\pm} = 200$  GeV and  $\tan\beta = 0.1$ .

## 4 Signal and background calculations

We perform the detailed simulation of the process (1) with the subsequent top quark decays into electron and muon ( $t \rightarrow be\nu_e$  and  $t \rightarrow b\mu\nu_\mu$ ) and relevant background reactions for three-year low luminosity run of LHC

$$\sqrt{s} = 14 \text{ TeV} \quad \text{and} \quad \int \mathcal{L} dt = 30 \text{ fb}^{-1}. \quad (10)$$

As an example we choose the values of the charged Higgs boson parameters as follows:

$$m_{H^\pm} = 200 \text{ GeV} \quad \text{and} \quad \tan\beta = 0.1. \quad (11)$$

Note, that our result is not very sensitive to the  $m_H$  value, however the chosen small value of  $\tan\beta$ , namely  $\tan\beta < 0.2$ , is important for further analysis.

For simulation of the signal process and the background reactions we use the **TOPREX 2.51** event generator [19]. At present the TOPREX provides the generation at the parton level the production of  $t\bar{t}$ -pair, three processes of single top ("Wg", "tW", and "W\*") and  $Wb\bar{b}$  production with subsequent top quark decay into  $bW$  and  $W$  into fermion anti-fermion pair. One can generate also several processes of top quark production via anomalous  $t$ -quark interactions [20].

We use the PYTHIA 6.134 [17] for simulation of quarks and gluons hadronization. We perform the simulation with taking into account of ability of CMS detector at LHC [14]. For "fast" detector simulation all events are passed through the package CMSJET 4.703 [18]. As a result the final event contains the information about momenta of "detected" photons, charged leptons ( $e, \mu$ ), hadronic jets and missing energy  $E_{T\text{mis}}$  (see [18] for details). The efficiencies for  $b$ -tagging of jets originating from  $b$ -quark,  $c$ -quark and light partons ( $u, d, s$ -quarks and gluon) are about 60%,

10%, and  $1 \div 2\%$ , respectively [18]. In what follows we refer the  $b$ -tagged jet as the  $B$ -jet.

For our choice of the  $H^\pm$ -boson parameters, (see (11)), the cross section for  $(t\bar{b} + \bar{t}b)$  production in the reaction (1) due to  $H^\pm$ -boson contribution at  $\sqrt{s} = 14$  TeV is equal to

$$\sigma(H^\pm) = 9.7 \text{ pb.} \quad (12)$$

There are several sources of the background to the considered process (1). We present here the cross section values of these processes evaluated at LO approximation. The consideration of the higher order corrections is given, for example, in [4]. These background processes are as follows (all cross section values imply the summation on particles and anti-particles):

- three processes of single top production

$$\begin{aligned} q\bar{q}' \rightarrow W^\pm \rightarrow t\bar{b}, \quad \sigma(W^*) &= 7.5 \text{ pb,} \\ gq \rightarrow q't\bar{b}, \quad \sigma(Wg) &= 180 \text{ pb,} \\ gb \rightarrow tW, \quad \sigma(tW) &= 60 \text{ pb} \end{aligned}$$

- $t\bar{t}$ -pair production:  $gg(q\bar{q}) \rightarrow t\bar{t}$ ,  $\sigma(t\bar{t}) = 600 \text{ pb}$
- $W b\bar{b}$  production:  $q\bar{q}' \rightarrow W b\bar{b}$ ,  $\sigma(Wb\bar{b}) = 360 \text{ pb}$
- $W + jets$  production (generated by PYTHIA)

$$\sigma(W + jets) = 59000 \text{ pb}$$

The signal process (1) and all background reactions (except  $W+jets$ ) are simulated by using of TOPREX generator. For evaluation of the last process ( $W+jets$ ) the PYTHIA parameter  $k_{T\min}$  is chosen to be equal to 2 GeV (i.e. CKIN(1)=2 [17]).

The process (1) of  $t\bar{b}$  pair production with subsequent top decay into  $bl\nu$  is characterized by presence in the final state of one charged isolated lepton (from  $W$ -boson decay), the missing energy (neutrino) and two hard  $B$ -jets from  $b$ -quarks.

The appropriate cuts providing a selection signal from the background processes, are considered in details in [4]. In particular, these cuts include the requirement of two “hard”  $B$ -jets:

$$\text{“hard” - cut : } p_T(B_1, B_2) \geq p_{T0} \sim 75 \text{ GeV} \quad (13)$$

However, this cut leads to essential modification of the form of corresponding  $\cos\vartheta^*$  distributions (9) of the top quark decay products.

Indeed, in Fig. 6 we present the angular distributions of the  $b$ -quark (from  $t$ -quark decay) evaluated at the parton level before and after cut on the  $b$ -quark

transverse momentum (see the histograms "b, c, f, g" in the Fig. 6). One can see that after application of the cut (13) the form of the angular distribution of  $b$ -quark, originating from the decay of right-handed  $t$ -quark (produced via  $H^\pm$  exchange) changes dramatically and even becomes qualitatively similar to that of  $b$ -quark from left-handed top decay (produced via  $W^+$  exchange). In view of actual possibilities of the detector it will be even more difficult to distinguish these two distributions.

Therefore, we propose another  $p_T$ -cut ("soft-hard") on the final  $B$ -jets. Namely, we require that  $p_T$  of one  $B_1$ -jet (from top quark) should not exceed of some value of  $p_{T1} = 100$  GeV, while  $p_T$  of the other  $B_2$ -jet should be greater then  $p_{T0} = 75$  GeV:

$$\text{"soft-hard" - cut : } p_T(B_1 \text{ from } t) \leq p_{T1} \text{ and } p_T(B_2) \geq p_{T0}. \quad (14)$$

It is seen from the histograms "d" and "h" in the Fig. 6 that this "soft-hard" cut (14) saves the forms of angular distributions of the decay products of  $t$ -quarks, produced through  $H^\pm$  and  $W^\pm$  exchange.

In further analysis we apply the both variants (13) and (14) of  $p_T$  cuts. Thus, for signal/background separation we require

1. one and only one isolated lepton (with  $p_T > 10$  GeV) and at least two hadronic jets (with  $p_T > 20$  GeV and pseudorapidity  $|\eta| < 4.5$ )
2. explicitly two  $b$ -tagged jets (with  $p_T > 25$  GeV and  $|\eta| < 2.5$ ) and no other hadronic jets
3. the transverse momentum of the reconstructed  $W$ -boson and two  $B_1$  and  $B_2$  jets should not exceed of 10 GeV,  $|\vec{p}_T(WB_1B_2)| \leq 10$  GeV
4.  $H$ ("hard")-cut on  $p_T$  of  $B$ -jets ( $p_T(B_1, B_2) \geq 75$  GeV)
- 4'.  $SH$ ("soft-hard")-cut on  $p_T$  of  $B$ -jets (one  $B_1$ -jet with  $p_T \leq 100$  GeV and second  $B_2$ -jet with  $p_T \geq 75$  GeV)
5. the reconstructed mass of the  $t$ -quark should be within  $150 \div 200$  GeV,  $|M_{rec}(BW) - m_t| < 25$  GeV

As usual, using the four-momentum of charged lepton and the transverse momentum of missing energy for reconstruction of  $W$ -boson momentum we get two solutions for  $p_{rec}(W)$ . For further reconstruction of top quark four-momentum,  $p_{rec}(t)$ , we should examine both two  $B$ -jets for the case of  $H$ -cut (13). As a result we obtain four combinations for reconstructed momentum of the  $t$ -quark. For  $SH$ -cut (14) we assume that the  $B_1$ -jet with the smallest transverse momentum is resulted from the  $t$ -quark decay and we have two solutions for  $p_{rec}(t)$ . Then, the invariant mass of the  $(WB)$ -system,  $M(WB)$ , with the value nearest to  $m_t = 173.8$  GeV is treated

as reconstructed value of the  $t$ -quark mass. The corresponding  $p_{rec}(t)$  is considered as reconstructed  $t$ -quark momentum.

The resulted efficiencies after application of all cuts to the signal and the background are given in the Table 1. One can see that new  $SH$  cut (14) provides slightly better efficiency for the signal reconstruction. However, the background suppression becomes also worth as compared to the application of old  $H$ -cut (13). The resulted number of reconstructed events (for  $\int \mathcal{L} dt = 30 \text{ fb}^{-1}$ ) and the corresponding signal-to-background ratios are given in the Table 2. It is seen that application of the old and new  $p_T$ -cuts result in almost the same  $S/B$  ratios. Therefore, the both two variants of  $p_T$ -cut ( $SH$  and  $H$ ) provide a rather well reconstruction of the top quark in the reaction (1).

The distributions on the reconstructed top quark mass are presented in the Fig. 7. The symbol “SM” corresponds calculations with the SM case, while the symbol “ $\text{SM}+H^\pm$ ” corresponds to the SM and  $H^\pm$ -boson contribution. The standard fit gives the following values of the reconstructed  $t$ -quark mass (in GeV):

	SM	$\text{SM} + H^\pm$
S-H	$172.4 \pm 11.8$	$171.6 \pm 11.4$
H	$172.8 \pm 11.2$	$172.4 \pm 10.8$

Now we proceed to separation of the  $H^\pm$ -boson contribution into the reaction (1). For this purpose we explore the difference in  $\cos \vartheta_l^*$ -distributions resulted from different polarizations of the  $t$ -quark, produced within the SM (only  $W$  exchange) and within  $W^\pm + H^\pm$  exchange (see Fig. 6). The distributions on  $\cos \vartheta_l^*$ , calculated for the sum of the signal and background events are given in the Fig. 9. The upper two histograms correspond to new  $SH$ -cut, while two lower histograms are obtained by application of old  $H$ -cut. We fit these distributions by linear dependence on  $\cos \vartheta_l^*$ :

$$\frac{dN}{d \cos \vartheta_l^*} \propto 1 + \alpha \cdot \cos \vartheta_l^* \quad (15)$$

The results of the fit is given in the Table 3. It is evident that the new  $SH$ -cut (14) is more sensitive to  $H^\pm$ -boson contribution. Indeed, the presence of charged Higgs leads to change of the sign of the slope of  $\cos \vartheta_l^*$ -distribution, while the application of the old  $H$ -cut leads only to modification of the slope  $\alpha$  (see Table 3).

Certainly, this result depends on the relative value of the  $H^\pm$ -boson contribution. Indeed, for larger value of the  $\tan \beta$  we should expect the decreasing of charged Higgs contribution and as a result the values of  $\alpha$  should be more close to SM expectations. Note, that for the large value of  $\tan \beta > 10$ , where we have a noticeable charged Higgs contribution, the produced top quark should be a left-handed. As a result, the angular distribution should be the same as in the SM case.

## 5 Conclusion

In the present article the contribution from charged Higgs bosons into the process of electroweak production of  $t\bar{b}$ -pair at LHC is considered and is analyzed in details. The expressions for matrix elements squared for the corresponding subprocesses are obtained and the role of the  $t$ -quark polarization is investigated. The cross sections and angular distributions at parton level are calculated. The simulation of the signal and relevant background processes by means of PYTHIA in view of opportunities of the CMS detector at LHC is also performed.

We show that the differential distributions ( $p_T$  and  $\eta$ ) of the  $t$ -quark and its decay products are practically the same as for the SM production of  $t\bar{b}$ -pair. As a result by using the conventional way for top quark separation from the background it would be difficult to distinguish the  $H^\pm$ -boson from  $W^\pm$ -boson exchange. At the same time the produced top quark through charged Higgs exchange has different polarization in comparison to the SM case. At small values of  $\tan\beta$ , one should expect the production of the right-handed  $t$ -quarks. The corresponding angular distributions of leptons essentially differ from those predicted by the SM.

In order to separate the  $W^\pm$  and  $H^\pm$  contributions into the reaction (1) we propose the new  $p_T$ -cut (14) for  $b$ -tagged hadronic jets. This “soft-hard”  $p_T$ -cut provides not only discrimination the signal for  $t$ -quark against the background processes, but also the selection of the contribution to the relevant process from a charged Higgs boson.

Certainly, the proposed  $p_T$ -cut may help only for the small values of  $\tan\beta < 0.2$ . For the larger values (i.e., for  $\tan\beta > 0.2$ ) one need to find another variables, which should be sensitive to charge Higgs boson contribution into the reaction (1). In principle, we may explore the SM prediction for the difference in top and anti-top quark production cross sections in the reaction (1). This difference results due to the absence of the valence anti-quark contributions in the proton-proton collisions [9, 13]. At the same time, the main contribution to the  $H^\pm \rightarrow t\bar{b}$  process comes from the interaction of charmed and strange quarks from initial hadrons. Since in the  $pp$ -collisions we have equal numbers of the  $c$ ,  $s$  quarks and anti-quarks, we should expect  $\sigma(H^+ \rightarrow t\bar{b}) \approx \sigma(H^- \rightarrow \bar{t}b)$ . Thus, the study of the asymmetry in  $t$ - and  $\bar{t}$ -quarks production in the reaction (1) may provide an additional possibility to separate the charged Higgs boson contribution.

### Acknowledgment

We thank to E. Boos, D. Denegri, V. Drollinger, V. Ilyin, A. Kostritsky, N. Krasnikov, M. Mangano, A. Nikitenko, V. Obraztsov, L. Sonnenschein, N. Stepanov, and T. Tait for fruitful discussions. The work of S.R.S. was supported, in part, by Russian Foundation for Basic Research, projects no. 99-02-16558.

## References

- [1] J.F. Gunion, H.E. Haber, G.L. Kane, and S. Dawson, “The Higgs Hunters’ Guide” (Addison-Wesley, Reading, MA, 1990).
- [2] R. Barate *et al.* [ALEPH Collaboration], CERN-EP-2000-086 [hep-ex/0008005];  
P. Abreu *et al.* [DELPHI Collaboration], Phys. Lett. **B460** (1999) 484;  
M. Acciarri *et al.* [L3 Collaboration], Phys. Lett. **B466** (1999) 71 [hep-ex/9909044];  
K. Ackerstaff *et al.* [OPAL Collaboration], Phys. Lett. **B426** (1998) 180 [hep-ex/9802004].
- [3] T. Affolder *et al.* [CDF Collaboration], Phys. Rev. **D62** (2000) 012004 [hep-ex/9912013];  
B. Abbott *et al.* [D0 Collaboration], Phys. Rev. Lett. **82** (1999) 4975 [hep-ex/9902028].
- [4] M. Beneke *et al.*, “Top quark physics,” hep-ph/0003033.
- [5] A. Djouadi *et al.*, “The Higgs working group: Summary report,” hep-ph/0002258.
- [6] A.C. Bawa, C.S. Kim, and A.D. Martin, Z. Phys. **C47** (1990) 75;  
V. Barger, R.J.N. Phillips, and D.P. Roy, Phys. Lett. **B324** (1994) 236;  
S. Moretti and K. Odagiri, Phys. Rev. **D55** (1997) 5627;  
J.F. Gunion, Phys. Lett. **B322** (1994) 125;  
F. Borzumati, J.-L. Kneur, and N. Polonsky, Phys. Rev. **D60** (1999) 115011;  
D. J. Miller, S. Moretti, D. P. Roy and W. J. Stirling, Phys. Rev. **D61** (2000) 055011 [hep-ph/9906230].
- [7] R. Kinnunen, J. Tuominiemi, and D. Denegri, *Search for the charged Higgs boson from top decays in CMS*, CMS TN/94-233 (1994).
- [8] S. Cortese and R. Petronzio, Phys. Lett. **B253**, (1991) 494;  
T. Stelzer and S. Willenbrock, Phys. Lett. **B357**, 125 (1995) [hep-ph/9505433].
- [9] A. P. Heinson, A. S. Belyaev and E. E. Boos, Phys. Rev. **D56** (1997) 3114 [hep-ph/9612424];  
A.S. Belyaev, E.E. Boos and L.V. Dudko, Phys. Rev. **D59**, 075001 (1999) [hep-ph/9806332].
- [10] T. Tait and C. P. Yuan, hep-ph/9710372;  
T. M. Tait, hep-ph/9907462;  
T. Tait and C. - Yuan, hep-ph/0007298.

- [11] M. Jezabek and J. H. Kühn, Nucl. Phys. **B320**, 20 (1989);  
 M. Jezabek, “Top quark physics,” Nucl. Phys. Proc. Suppl. **37B**, 197 (1994) hep-ph/9406411.
- [12] G. Mahlon and S. Parke, Phys. Rev. **D55**, 7249 (1997) hep-ph/9611367;  
 G. Mahlon and S. Parke, Phys. Lett. **B476**, 323 (2000) [hep-ph/9912458];  
 E. L. Berger and T. M. Tait, hep-ph/0002305;  
 C. A. Nelson and L. J. Adler, hep-ph/0007086.
- [13] G. V. Jikia and S. R. Slabospitsky, Phys. Lett. **B295** (1992) 136.
- [14] CMS Technical Proposal, CERN/LHC/94-43 LHCC/P1 (1994).
- [15] H. L. Lai *et al.* [CTEQ Collaboration], Eur. Phys. J. **C12** (2000) 375 [hep-ph/9903282].
- [16] *Review of particle physics*, D.E. Groom *et al.*, Eur. Phys. J. **C15** (2000) 1.
- [17] T. Sjöstrand and M. Bengtsson, Comput. Phys. Comm. **43** (1987) 367;  
 T. Sjöstrand, *PYTHIA 5.7*, Comput. Phys. Comm. **82** (1994) 74.
- [18] S. Abdullin, A. Khanov and N. Stepanov, *CMSJET*, CMS TN/94-180 (1999).
- [19] S.R. Slabospitsky *et al.*, CMS Technical Note, in preparation.
- [20] Y. P. Gouz and S. R. Slabospitsky, Phys. Lett. **B457** (1999) 177 [hep-ph/9811330].

Table 1: The efficiencies (in %) of the signal ( $H^\pm$ ) and background separation after application of cuts. The symbols  $SH$  and  $H$  correspond to usage of the new (14) and old (13)  $p_T$ -cut

	$H^\pm$	$W^\pm$	$Wg$	$Wt$	$t\bar{t}$	$Wbb$	$W + \text{jets}$
SH	0.77	0.5	0.012	0.008	0.003	0.02	$5 \cdot 10^{-5}$
H	0.26	0.4	0.007	0.003	0.003	0.01	–

Table 2: The number of events, resulted after application of all cuts. In the calculations the total integrated luminosity of  $\int \mathcal{L} dt = 30 \text{ fb}^{-1}$  is assumed. The symbols  $W/B$  and  $H/B$  correspond to signal-to-background ratios, calculated within the SM framework as well as for the SM and  $H^\pm$ -boson contribution, respectively. The symbol SH(H) stand for usage of the new (old)  $p_T$ -cut.

	$H^\pm$	$W^\pm$	SM	SM + $H^\pm$	$\frac{W}{B}$	$\frac{H}{B}$
SH	470	260	960	1430	0.37	0.49
H	260	220	610	870	0.55	0.43

Table 3: The result of the fit of  $\frac{dN}{d\cos\theta_l^*}$  distribution by the function of  $(1 + \alpha \cdot \cos\theta_l^*)$ . The symbol “SM” corresponds calculations with the SM case, while the symbol “SM+ $H^\pm$ ” corresponds to the SM and  $H^\pm$ -boson contribution.

	$\alpha(\text{SM})$	$\alpha(\text{SM} + H^\pm)$
SH	$-0.29 \pm 0.06$	$+0.21 \pm 0.05$
H	$-0.98 \pm 0.05$	$-0.46 \pm 0.06$

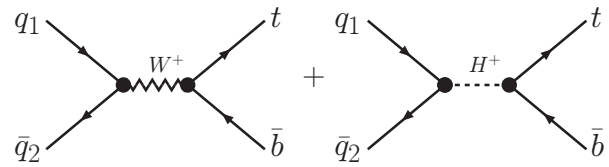


Figure 1: Feynman diagrams for the subprocess  $q_1\bar{q}_2 \rightarrow (W^\pm H^\pm) t\bar{b}$

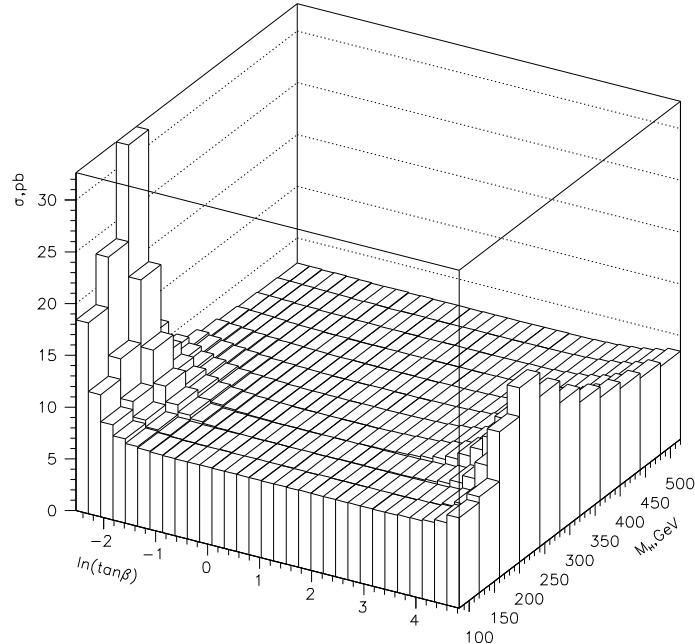


Figure 2: The behavior of the total cross section for  $(t\bar{b} + \bar{t}b)$ -pair production in  $pp$ -collision at  $\sqrt{s} = 14$  TeV as a function of  $\tan\beta$  and charged Higgs mass  $m_H$ .

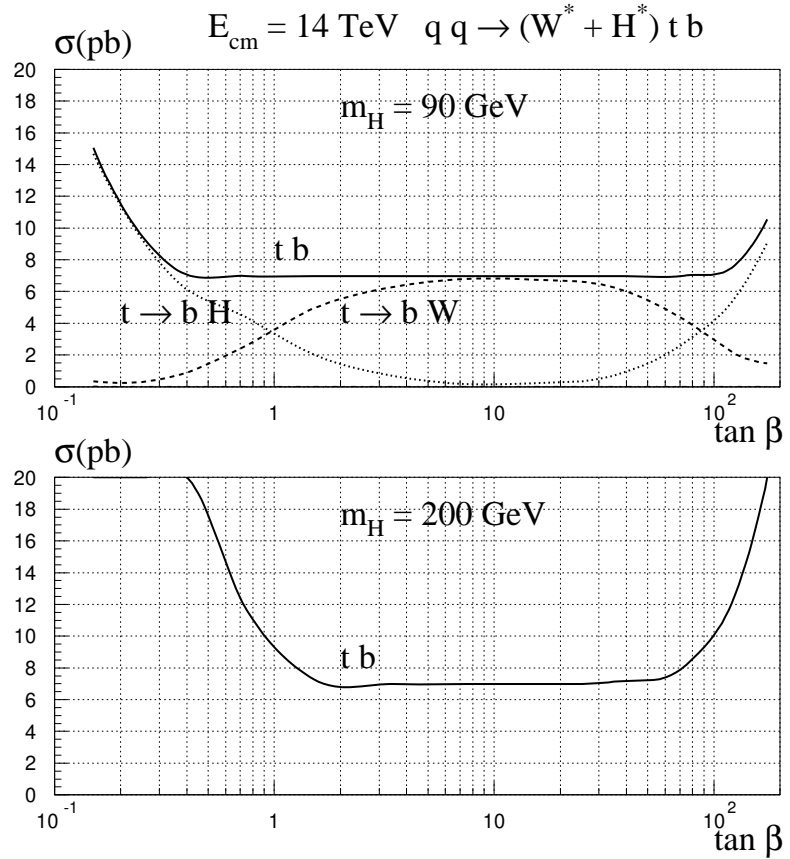


Figure 3: The dependence of the  $(t\bar{b} + \bar{t}b)$ -pair production cross section versus  $\tan \beta$  for two values of  $m_H = 90$  and  $200$  GeV (the solid curves). The dashed and dotted curves correspond to the cross section production times the branching ratio of  $t$ -quark decays into  $bW^\pm$  and  $bH^\pm$ , respectively.

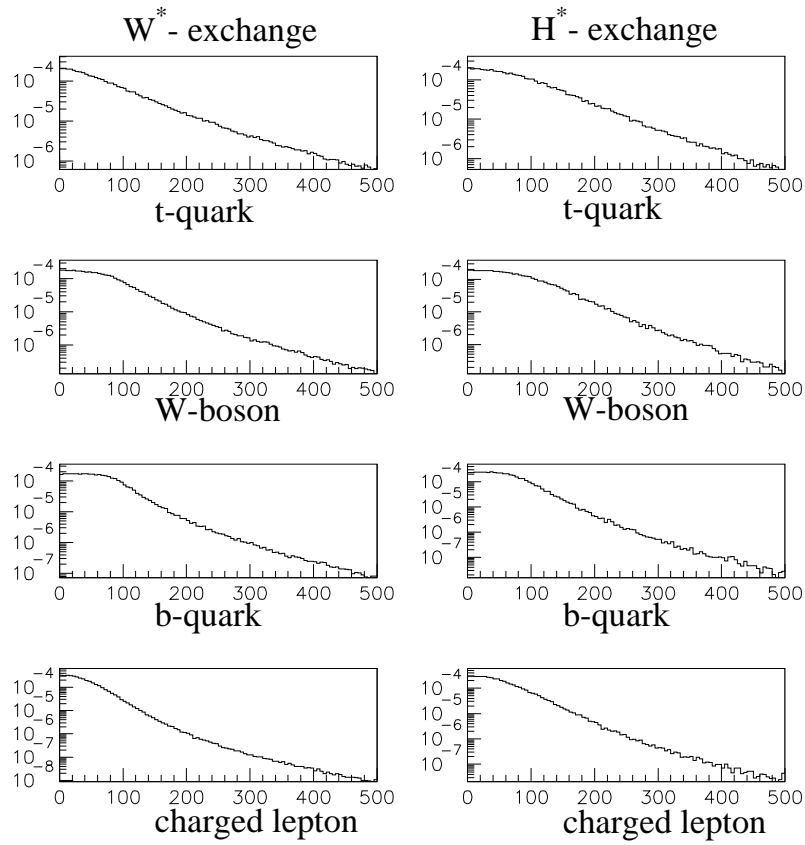


Figure 4: The  $p_T$ -distribution of the top quark and the products of its decay  $t \rightarrow bW(\rightarrow b\ell\nu)$  produced in the reaction (1).  $\frac{d\sigma}{dp_T}$  is in arbitrary units, while  $p_T$  (the  $x$ -axis) is in GeV. The symbol  $W^*$  ( $H^*$ ) corresponds to  $t\bar{b}$ -pair production through  $W^\pm$  ( $H^\pm$ )-exchange only.

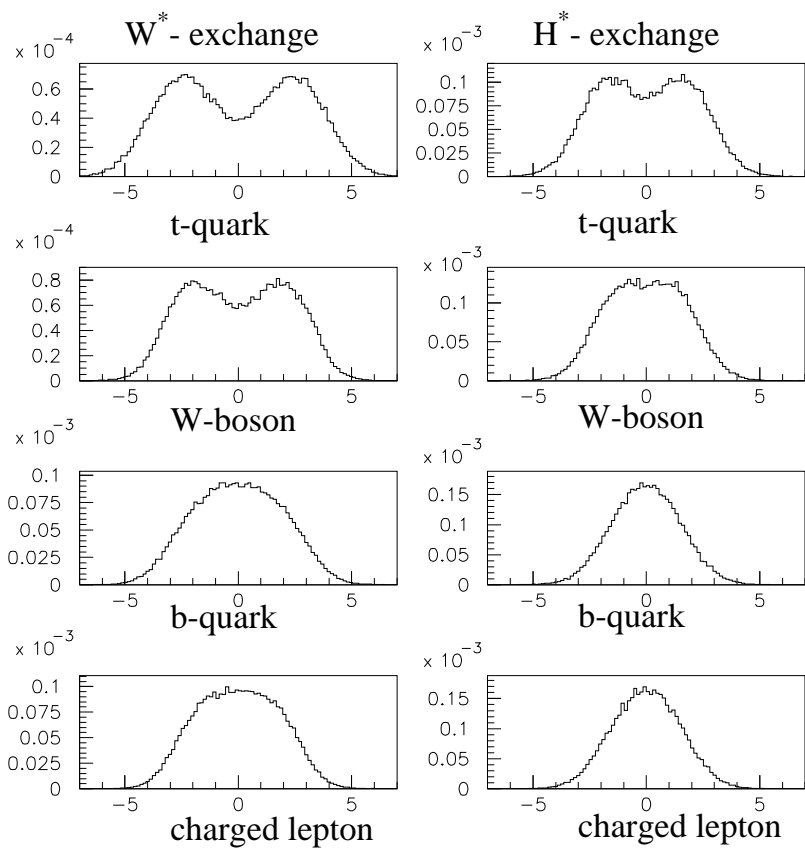


Figure 5: The pseudorapidity,  $\eta$ , distributions of the  $t$ -quark and its decay products. For additional explanation see previous Fig.4.

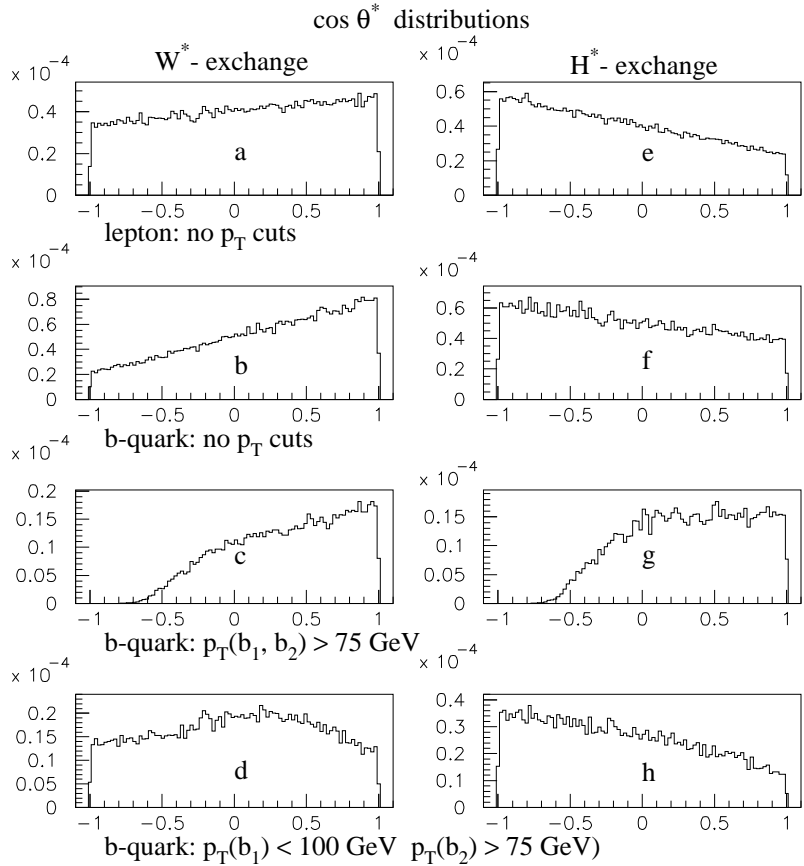


Figure 6: The  $\cos \vartheta^*$ -distributions of the charged lepton and  $b$ -quark originating from the  $t$ -quark decay. All distributions are obtained from the evaluation of the reaction (1) at the parton level for  $W^\pm$ -boson exchange ( $W^*$ ) and  $H^\pm$ -boson contribution ( $H^*$ ). The histograms “a, b, e, f” are obtained without any cuts. The H-cut (13) and SH-cut (14) are used for production of “c, g” and “d,h” histograms, correspondingly.

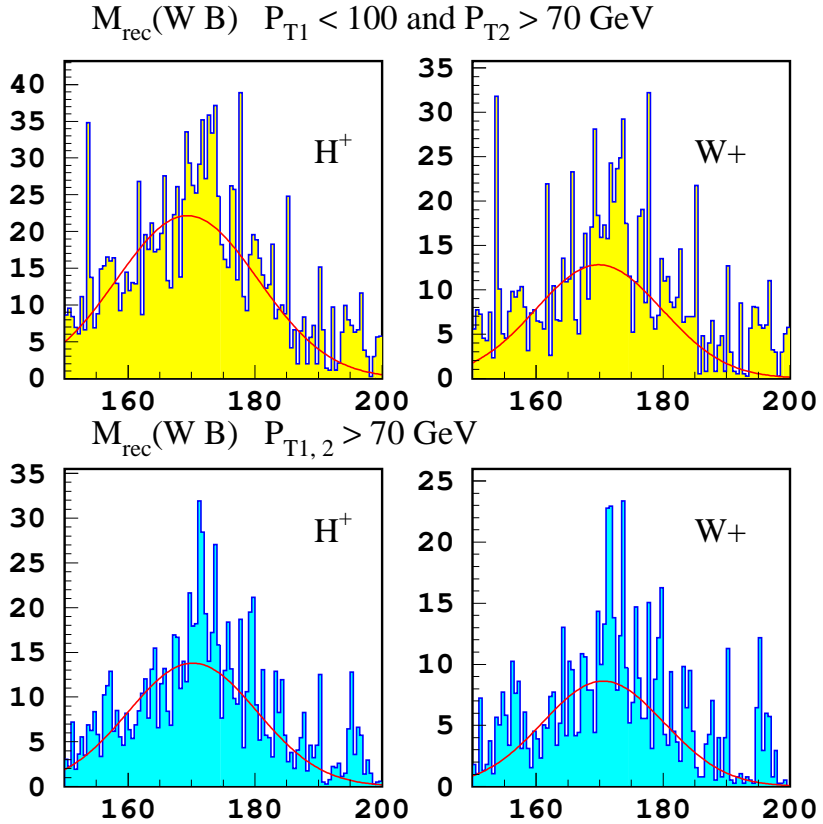


Figure 7: The distributions (in the arbitrary units) on the invariant mass of the  $(W B)$ -system,  $M_{rec}$  (in GeV) resulted after application of all 1–5 cuts. Two upper and lower histograms correspond to application of the new SH-cut (14) and old H-cut (13), respectively. The symbol  $W^+$  corresponds to the SM and background processes, while the symbol  $H^+$  refers to the  $H^\pm$ , the SM and background contributions.

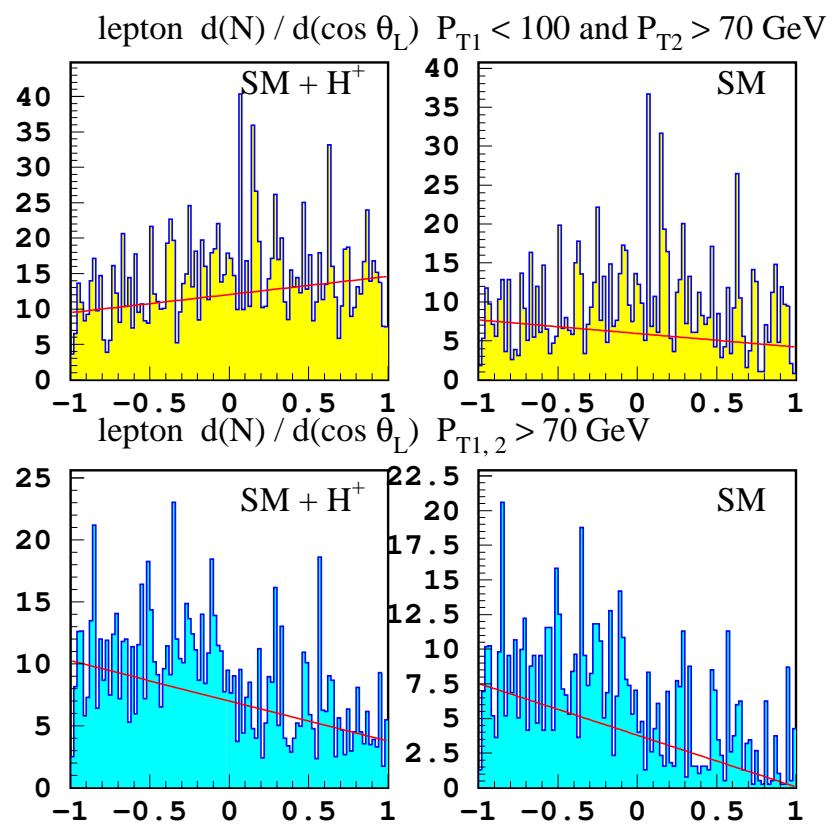


Figure 8: The  $\cos \vartheta^*$ -distributions for charged lepton. The lines correspond to the fit to linear dependence of (15).